ELSEVIER

Journal of Structural Geology 26 (2004) 2145–2156

JOURNAL OF STRUCTURAL GEOLOGY

www.elsevier.com/locate/jsg

Controls on the geometry of tails around rigid circular inclusions: insights from analogue modelling in simple shear

Santanu Bose[a], Fernando O. Marques[b,*]

[a]*Research Project GEOMODELS and CGUL, Faculdade de Ciências, Universidade de Lisboa, Edifício C8, Piso 6, 1749-016 Lisboa, Portugal*
[b]*Departamento Geologia and CGUL, Faculdade de Ciências, Universidade de Lisboa, Edifício C8, Piso 6, 1749-016 Lisboa, Portugal*

Received 15 January 2004; received in revised form 10 May 2004; accepted 15 May 2004
Available online 19 August 2004

Abstract

We used analogue modelling to investigate the factors controlling tail geometry in porphyroclast systems. Results show that: (1) σ inclusions can develop in both slipping and non-slipping modes, but δ-inclusions only form in the latter. (2) σ inclusions develop when the mantle production rate is constant and the mantle is transected by the separatrix. δ inclusions form when the mantle is initially outside the separatrix and later comes inside this line. (3) In the slipping mode, the wedge-shaped tail of σ-inclusions always has a straight external surface parallel to the shear plane, whereas in the non-slipping mode the external surface is curved inwards (external embayments). (4) Together with earlier theoretical results, σ- and δ inclusions always show stair-stepping of tails when embedded in a viscous matrix under homogeneous simple shear deformation. (5) Maximum stair-stepping occurs in the slipping mode and is at least equal to the inclusion diameter. If our models bear significant similarity to nature, then (i) the straight or curved character of σ-inclusions could mean that they had, respectively, a slipping or non-slipping interface with the surrounding recrystallized matrix, and (ii) δ-inclusions may result from shear deformation under retrogressive metamorphic conditions in thrust systems.

Keywords: Tail geometry; σ- and δ-inclusions; Non-slipping and slipping modes; Viscous matrix; Flow patterns; Analogue modelling

1. Introduction

A great deal of the deformation observed in rocks is concentrated in relatively narrow high strain zones that may affect the entire lithosphere. They accommodate considerable amounts of shortening and transcurrent movement in orogenic belts, and of extension in rifting lithosphere. Mylonites are the deep-seated expression of these shear zones. Therefore, it is essential to understand the flow of rocks in mylonite zones to accurately model the rheology of the lithosphere. Mylonitic rocks often contain mantled porphyroclasts, which are defined by the presence of weakly deformed to undeformed cores surrounded by softened material. The mantle material is formed either by the process of dynamic recrystallization along the outer rim of the undeformed core or by reaction softening such as the formation of mica and quartz from feldspar (Tullis and Yund, 1985; Passchier and Simpson, 1986). The formation of tail structures results from deformation of the mantle around a rigid core in response to the ductile flow in the surrounding matrix (Passchier and Simpson, 1986). The geometry of structures associated with rigid clasts in mylonites can be an important source of information on their kinematics and mechanical behaviour. Porphyroclast systems and similar structures have been commonly used to deduce the sense of shear in mylonites and, therefore, they have received a great deal of attention in recent decades (e.g. Burg et al., 1981; Simpson and Schmid, 1983; Passchier and Simpson, 1986; Choukroune et al., 1987; van den Driessche and Brun, 1987; Hanmer and Passchier, 1991; Passchier and Sokoutis, 1993; Passchier, 1994; Bjørnerud and Zhang, 1995; Masuda and Mizuno, 1996a; Mandal et al., 2000). The geometry of porphyroclast systems has also been used to try and deduce rock properties (e.g. Passchier et al., 1993; Bons et al., 1997).

Passchier and Simpson (1986) concluded that the ratio

* Corresponding author. Tel.: +351-217500000; fax: +351-217500064
E-mail address: fmarques@fc.ul.pt (F.O. Marques).

0191-8141/$ - see front matter © 2004 Elsevier Ltd. All rights reserved.
doi:10.1016/j.jsg.2004.05.004

between mantle production rate ($\dot{R}$) and deformation rate ($\dot{\gamma}$) could be the most important factor controlling the geometry of tails associated with a rigid circular inclusion. However, they could only obtain a δ-inclusion when $\dot{R}/\dot{\gamma}$ was equal to zero, i.e. when $\dot{R}=0$, meaning that an instantaneous mantle was present in the initial stage and lay partially outside the separatrix. When $\dot{R}/\dot{\gamma}$ was different from zero, a σ-type system was produced, but the relative position between mantle and separatrix was not mentioned. Masuda and Mizuno (1996a) concluded that matrix rheology (Newtonian or non-Newtonian power-law) does not greatly influence the porphyroclast type, which is then determined by the radius of an initial circular mantle around the circular inclusion, in viscous simple shear flow. Mandal et al. (2000) concluded that the factor governing the geometry of mantle structures in simple shear is the rate of clast-size reduction for the case of a circle. With our investigation, we show that there are other factors controlling the geometry of tails around rigid inclusions.

The flow of a viscous matrix around a rigid inclusion to which it is adherent has been the subject of several studies. The main conclusions do not currently appear to be consensual: for instance, Cox et al. (1968), Masuda and Ando (1988) and Masuda and Mizuno (1996b) showed theoretically that the flow around a circular rigid inclusion has an eye-shaped pattern (Fig. 1A), but ten Brink and Passchier (1995), Bons et al. (1997), Pennacchioni et al. (2000) and Samanta et al. (2003) showed, experimentally and theoretically, that it has the shape of a bow tie (Fig. 1B). These differences could be the result of using different boundary conditions, as pointed out by Bons et al. (1997), although all mentioned studies are in simple shear. Pennacchioni et al. (2000) analysed the effect of a slipping boundary between inclusion and matrix in the flow pattern, and concluded that it is double bulge-shaped (similar to eye-shaped) in the slipping mode. Marques and Bose (2004) investigated experimentally the effect of a slipping matrix/inclusion interface and found a flow pattern different from the bow tie and eye-shaped patterns.

Ildefonse and Mancktelow (1993), Marques and Cobbold (1995), Marques and Coelho (2001), Pennacchioni et al. (2000), Mancktelow et al. (2002), Schmid (2002) and Ceriani et al. (2003) showed that a low-friction boundary between inclusion and matrix considerably changes the rotation behaviour of rigid inclusions.

Despite the great efforts put forth by former theoretical and experimental investigations, the conditions controlling geometry of tails around rigid inclusions in viscous simple shear and their meaning are still not well understood. Therefore, in this study, we concentrate our investigation on the geometry of tails around rigid inclusions in the non-slipping and slipping modes, and the relationship with the flow patterns in the surrounding matrix. Our investigation also focused on the effects of stability of mantle production rate and its position relative to the separatrix on the geometry of tails. We carried out analogue experiments with inclusions either adherent (polymer) or non-adherent (ice) to the viscous matrix (polydimethyl-siloxane—PDMS) in homogeneous simple shear.

2. Experimental procedure

2.1. Boundary conditions

The experiments were carried out in the parallel-sided simple shear rig used by Marques and Coelho (2001), because we wanted to analyse structures and flow in natural parallel-sided shear zones. Experiments took place at room temperature (ca. 18 °C), and at a constant far-field strain rate of ca. $1.25\times10^{-3}\ s^{-1}$ in the non-slipping mode and ca. $6.25\times10^{-3}\ s^{-1}$ in the slipping mode. According to Weijermars (1986), these values fall in the interval appropriate for geological laboratory experiments with linear viscous materials. To assure homogeneous simple shear, PDMS sticks to the walls that drive simple shear flow (parallel to the shear plane) and is non-adherent to the remaining four walls. The ice inclusion rotates freely inside PDMS, but the polymer inclusion strongly adheres to PDMS.

PDMS is a poor thermal conductor (0.002 W mK^{-1}) and the experiments have short-term duration. Therefore, the possible effects of low temperature induced by the ice on the polymer viscosity are restricted to a thin layer adjacent to the inclusion. Note that PDMS slides past the inclusion and, thus, the effects of low temperature on viscosity are only transient.

2.2. Experimental set up

The analogue materials used were a transparent polydimethyl-siloxane (PDMS—manufactured by Dow Corning of Great Britain under the trade name SGM 36) as the viscous matrix (see Weijermars (1986) for PDMS properties), already used in earlier experimental investigation with similar constraints (e.g. Passchier and Simpson, 1986; Passchier and Sokoutis, 1993; Marques and Cobbold, 1995; Arbaret et al., 2001; Marques and Coelho, 2001; Rosas et al., 2002; Mancktelow et al., 2002), and polymer or ice as rigid inclusions to simulate, respectively, non-slipping and slipping interfaces with the matrix. Both the ice and polymer inclusions have similar densities to that of the PDMS matrix, and so undesirable effects of gravity on the inclusion were null. We concentrated the study on cylindrical inclusions with circular cross-sections in the XZ plane (perpendicular to the vorticity axis), because (i) our aim is not the study of rolling structures in the non-slipping mode (as defined by van den Driessche and Brun (1987) for shapes other than circles), and (ii) in the slipping mode all inclusion shapes come to a stable orientation and the final geometry of tails is similar to that of the circle. The inclusions were mostly cylinders of 25 mm length, with a basal radius of 10 mm, but rectangular or rhombus prisms

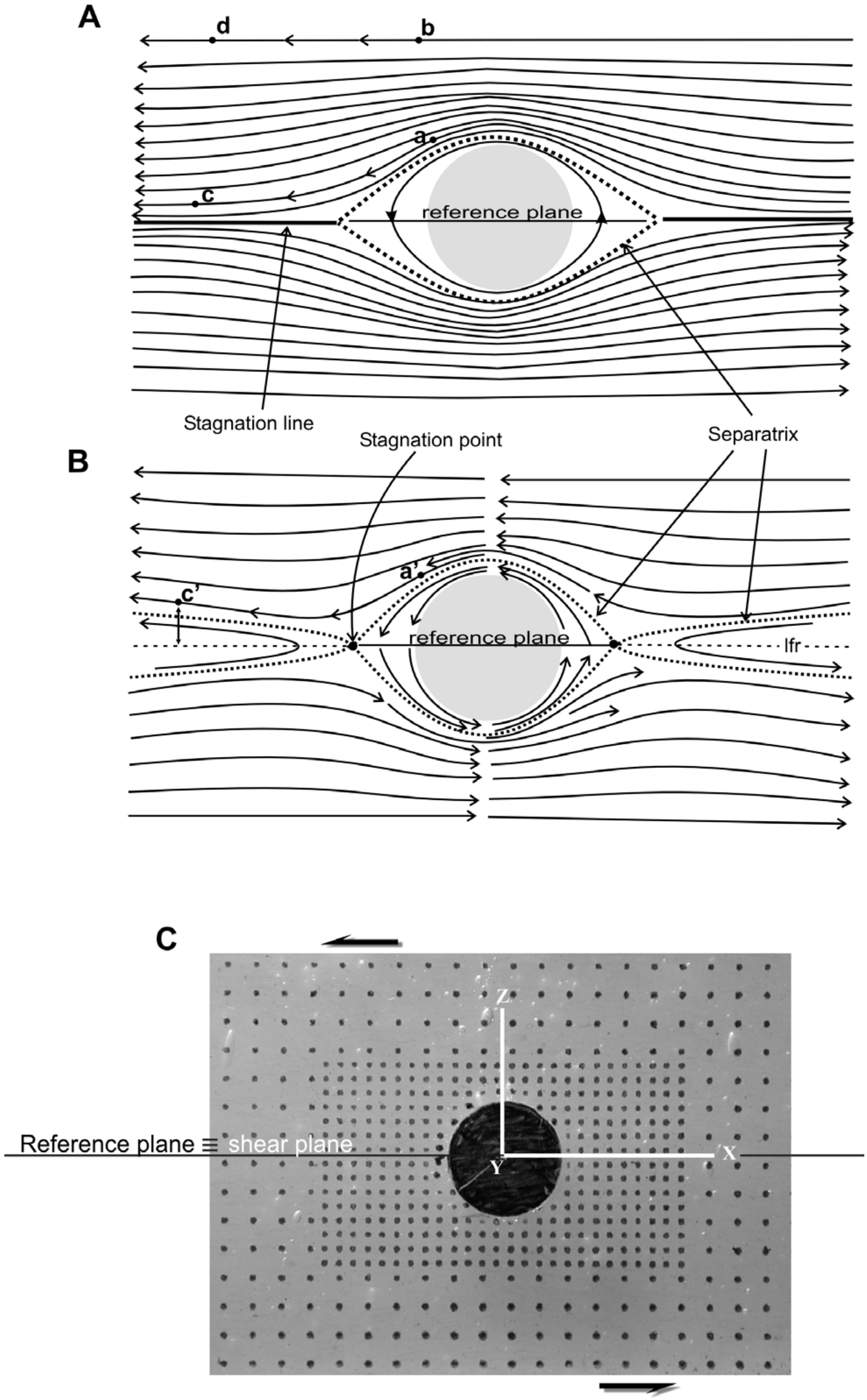

Fig. 1. Schematic representation of perturbation of streamlines around a rigid circle in the *XZ* plane. (A) Eye-shaped pattern. (B) Bow tie-shaped pattern. The separatrix is a line separating open from closed streamlines. Line of flow reversal (LFR) is the line along which the sense of flow is reversed. Note that: (i) material points following open stream lines can never cross the separatrix and/or the reference plane, implying that stair-stepping must always exist if the mantle has been outside the separatrix in some stage of deformation; (ii) material points born in similar positions relative to the inclusion crests in (A) and (B) (a and a', respectively) show a more prominent stair-stepping in the bow tie-shaped pattern (distance of points c and c' from the reference plane). (C) Reference frame used in the models, over photograph of *XZ* plane of initial stage.

and elliptical cylinders 25 mm high, with greatest principal axis equal to 30 mm and least principal axis equal to 20 mm (aspect ratio equal to 1.5) were also used. In our experiments, the ice melted about 20% in the basal area in about 8 min, but melt took place in the whole inclusion surface. A thin film of liquid water is always present in the inclusion/matrix boundary that guarantees permanent free slip. Water does not react chemically or mix with PDMS.

We stamped a grid on the PDMS matrix (Fig. 1C) to better visualize flow and strain in the matrix, and put a passive, black-coloured circular ring around the rigid body to model the recrystallized mantle in the non-slipping mode. For each experiment, a rectangular cake of PDMS 500 mm long, 80 mm wide and 30 mm high, with the rigid inclusion embedded in the middle, was placed between two parallel moving walls with no slip and two articulated walls with free slip. Photographs were taken at regular intervals ($\gamma = 0.125$) to record the flow of matrix around the rigid body. Displacements within the matrix were determined by superimposing photographs of regular intervals and drawing the paths followed by individual particles of the stamped grid. The finite deformation of the stamped grid indicates that deformation within the matrix was under homogenous simple shear.

3. Experimental results

3.1. Slipping mode

The results of experiments with slipping ice inclusions are presented in Figs. 2A and 3. In these experiments we did not use a passive circular marker around the rigid body to serve as a mantle, because melting water acted as a thin mantle around the inclusion. The melting of ice with progressive deformation is the analogue to the natural process of constant rate of mantle production and clast reduction by dynamic recrystallization or reaction softening. Melted water acts as a mantle, which is much less viscous than PDMS and, therefore, is squeezed out to pressure shadows and tails. Nevertheless, water is permanently present and guarantees free slip. The major observations related to these experiments are:

(i) The flow around the rigid circle has an overall shape that is neither bow tie nor eye-shaped (Marques and Bose, 2004).
(ii) Streamlines and passive marker lines show a rectilinear character parallel to *X* near the inclusion crests.
(iii) The matrix close to the inclusion facing the extensional quadrants does not go with the inclusion; instead, it tends to follow the bulk extensional direction. In the contraction quadrants of simple shear, there is splitting of the streamlines at the inclusion surface. We did not observe stagnation points on each side of the inclusion or closed displacement paths surrounding the inclusion.
(iv) Together, ice and liquid water develop the geometry of a σ-type inclusion (Figs. 2A and 3), with tails of liquid water in the form of wedges with characteristic planar external surfaces (those facing shear zone walls) and curved internal surfaces. The tails show prominent stair-stepping, at least equal to the inclusion diameter.
(v) The tails develop in the extension quadrants and are filled with liquid water squeezed out from the ice surface in the contraction quadrants.

3.2. Non-slipping mode

3.2.1. Flow pattern

Fig 2B shows the result of experiments with a rigid cylindrical inclusion adherent to the matrix. The flow pattern around the inclusion is bow tie-shaped and markedly different from that of the slipping mode. The observation of the final result shows that:

(i) The matrix close to the rigid circle rotates with the rigid inclusion to form a field of closed elliptical flow lines. This elliptical domain is separated from the open flow lines by a boundary called the separatrix. There are two stagnation points in the flow at the ends of the longest axis of the elliptical domain (black dots on both sides of the inclusion in Fig. 2B).
(ii) Strain around the rigid inclusion is highly heterogeneous, in contrast with the slipping mode.
(iii) Contrary to the slipping mode, perturbation of streamlines and passive marker lines near the inclusion crests is considerable, even at significant distances from the rigid body.

3.2.2. Tail geometry

Our experimental results show that two main types of tail geometry can develop in simple shear with adherent inclusions: σ- and δ-types.

3.2.2.1. σ-type tail geometry. Fig. 4A shows the experimental development of a σ-type inclusion in the non-slipping mode. In this case, the thickness of the mantle was kept constant throughout deformation around the rigid inclusion, with the mantle always transected by the separatrix. To keep a constant mantle width, we put a ring of passive marker around the rigid body at constant intervals. The thickness of the mantle was chosen in accordance with the theoretical analysis of Masuda and Mizuno (1996a,b) for the position of the separatrix. The reasons for using a passive marker around the porphyroclast without reducing the size of the rigid body are: (a) mantle material and matrix are presumed to be of similar rheology (non-slipping mode) and (b) the size of the separatrix reduces proportionally with the reduction of the rigid body (Passchier, 1994).

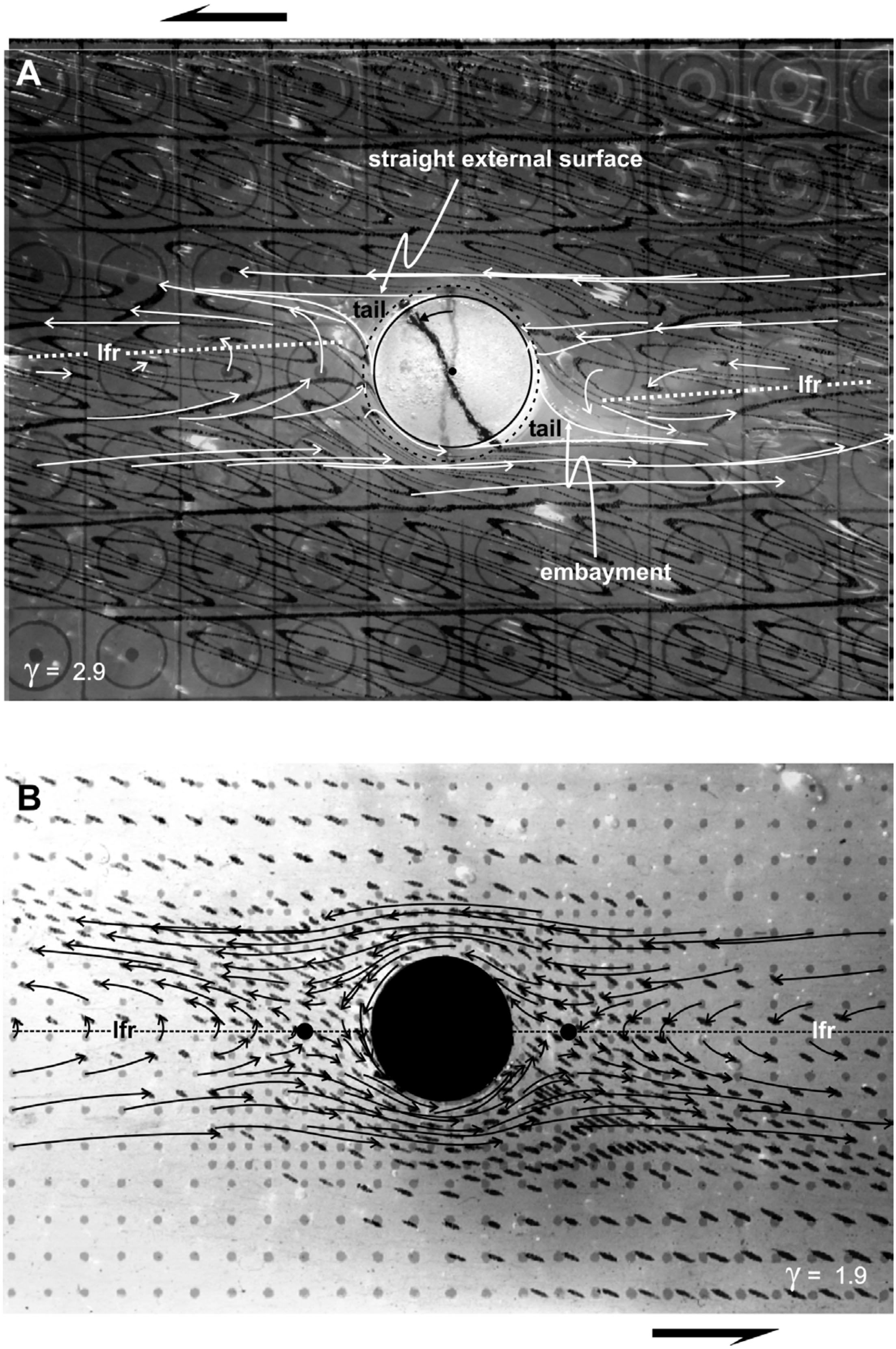

Fig. 2. Photographs of the *XZ* plane of final results of experiments in the slipping (A) and non-slipping (B) modes. The black dots on both sides of the circle in (B) are the stagnation points. Note that they seem to be absent in the slipping mode. Also note the rectilinear character of streamlines and external surfaces of the wedge-shaped tails in (A) and the prominent curvature of streamlines close to the inclusion crests in (B), and compare with the natural examples in Fig. 5A and B.

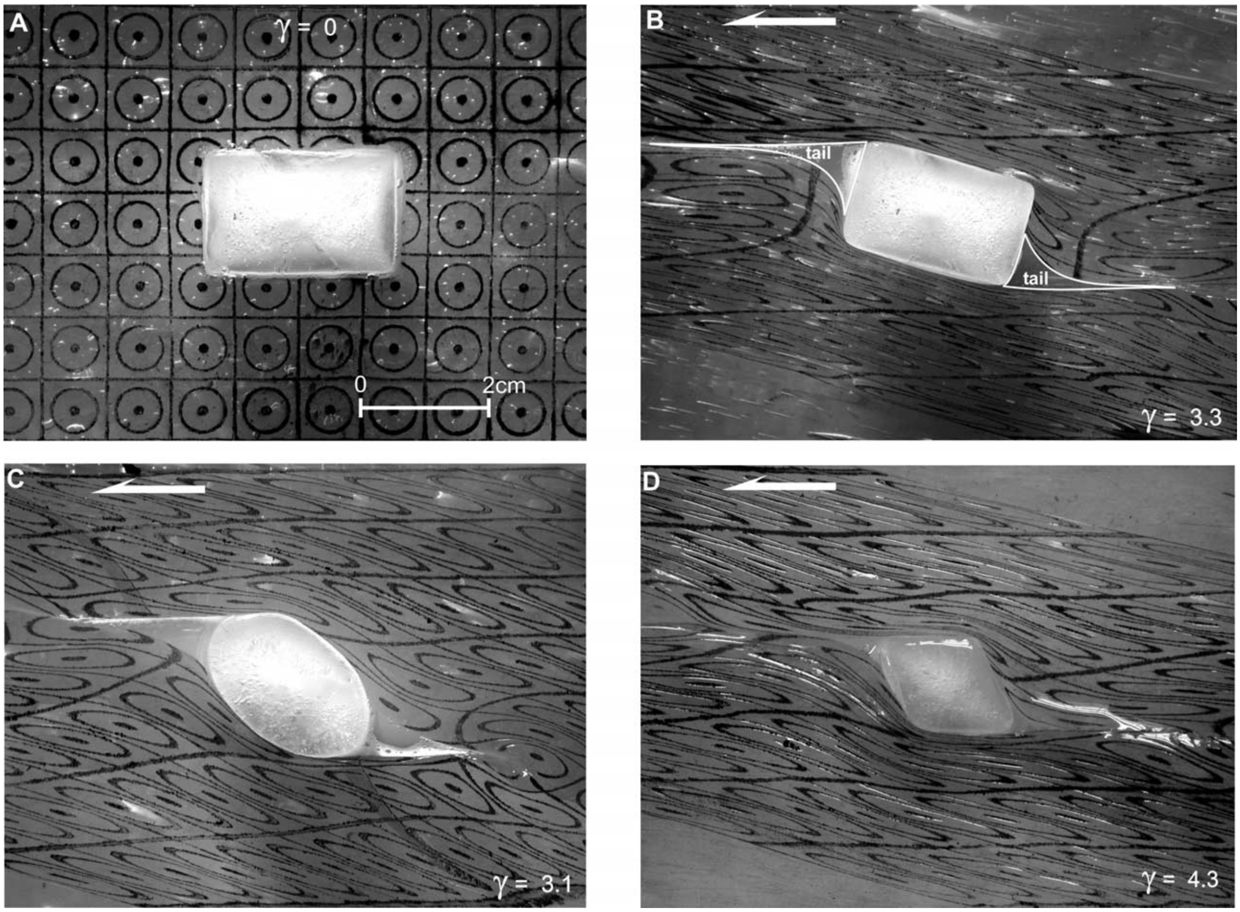

Fig. 3. Photographs of the *XZ* plane of results of experiments in the slipping mode for inclusions with shapes different from the circle. (A) Initial stage of the rectangular inclusion with greatest principal axis parallel to the shear direction. This is also the initial orientation of the elliptical and rhombus inclusions in (C) and (D). (B)–(D) Final stages showing σ-geometry with high degree of stair-stepping for all inclusion shapes.

Comparison of Figs. 4A and 1B indicates that the mantle segment outside the separatrix flows in open flow paths, whereas the mantle segment inside the separatrix rotates in elliptical closed flow paths. The result is the development of a σ-inclusion with curved external surfaces of the wedges (external embayment), in contrast with the slipping mode. By definition, in the case of a σ-clast, this external embayment does not cross the reference plane. The model tails show prominent stair-stepping.

3.2.2.2. δ-type tail geometry. Fig. 4B shows the development of a δ-type inclusion in the non-slipping mode. In this case, the mantle production rate was made heterogeneous: in the early stages of deformation, the mantle was kept outside the separatrix and with a constant thickness, and later the mantle production was stopped, which brought it inside the separatrix. The final stage at $\gamma = 6$ shows tails with prominent stair-stepping and external embayments that cross the reference plane. The tails of the experimental δ-inclusion are always at an angle with the shear plane, although this angle decreases at the tips with deformation, as a result of streamline configuration close and away from the inclusion.

4. Discussion of results

4.1. Flow pattern

Our experiments were carried out in two distinct modes, non-slipping and slipping, and the results reflect these differences. The overall flow pattern is neither bow tie nor eye-shaped, and shows significant differences in the detail. In the slipping mode (Fig. 2A), the nearby matrix flows past the inclusion, which reflects the very low friction between viscous matrix and rigid inclusion in the experiments, whereas in the non-slipping mode the nearby matrix flows with the inclusion, which reflects the dominant effect of viscous drag in this mode. Therefore, in the non-slipping mode, passive marker lines parallel to *X* and flow lines show considerable deflections at the inclusion crests, in great contrast with the slipping mode where they remain mostly straight. This has great influence in the shape of tails as discussed below. In the slipping mode we did not observe closed flow lines surrounding the inclusion, which means that there is no separatrix around the inclusion The flow of the matrix around the rigid inclusion becomes, therefore, crucial for understanding the geometry of tail structures

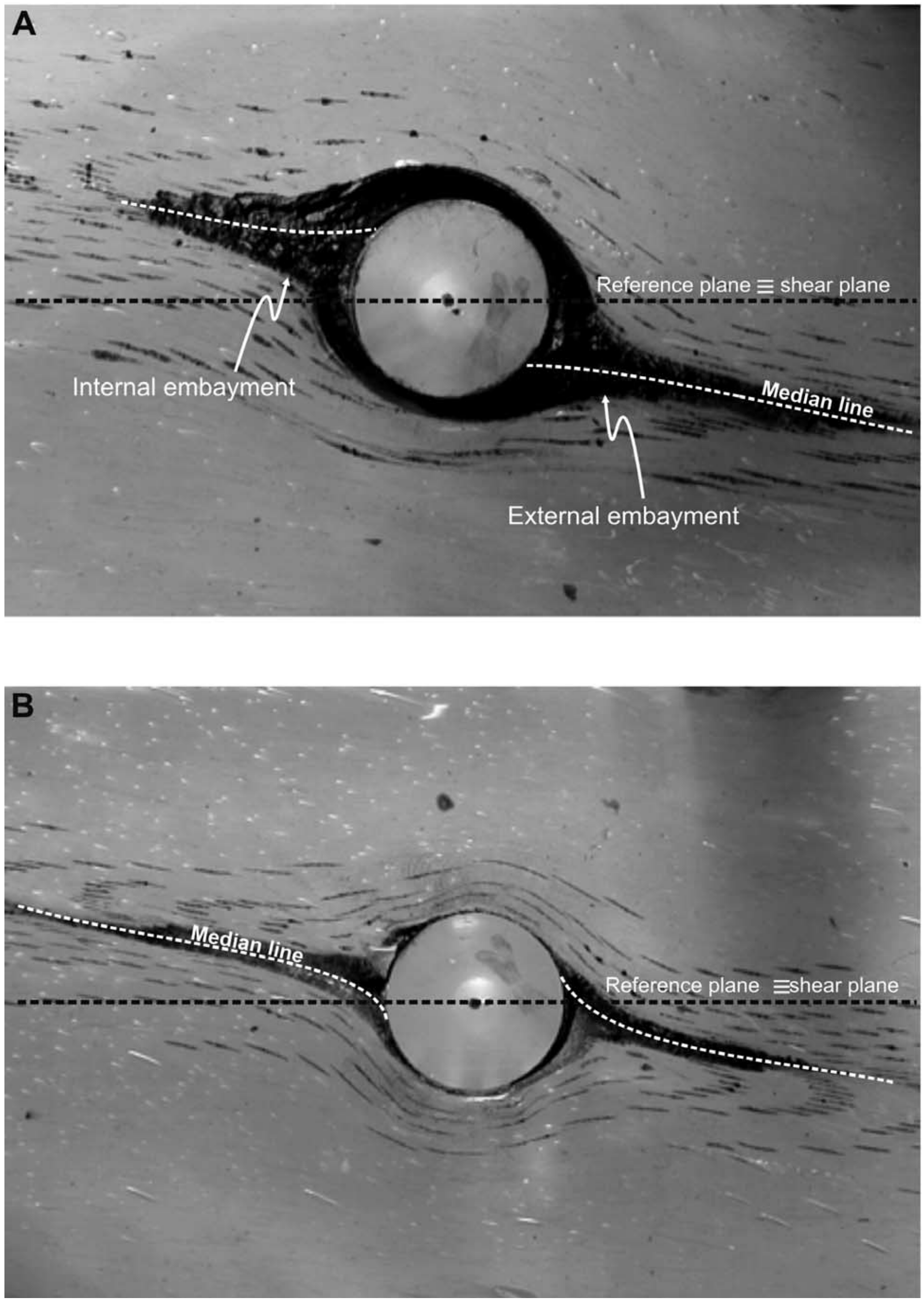

Fig. 4. Photographs of *XZ* sections of final results of experiments in the non-slipping mode. (A) σ-inclusion formed due to constant rate of mantle production, which is permanently transected by the separatrix. Note the curved external surfaces of the tails in (a) and compare them with their straight character in Fig. 2A. (B) δ-inclusion formed by heterogeneous rate of mantle production, i.e. early mantle transected by separatrix and later drastic reduction of mantle to bring it inside the separatrix.

associated with rigid bodies in mylonites of ductile shear zones.

4.2. Tail geometry in the slipping mode

Our experiments in this mode show that simple shear always produces σ-clasts with wedge-shaped tails, independently of inclusion shape and/or aspect ratio (Figs. 2A and 3). The rectilinear character of the external surfaces of the wedges (those facing shear zone walls) is the result of the shear-parallel streamlines at the inclusion crests (cf. streamlines in Fig. 2A). The concave geometry of the internal parts of the wedges (internal embayments) results from the shape of the flowing matrix. The pressure shadows and tails are filled with liquid water squeezed out from the ice surface in the contraction quadrants. The tails work as local shear parallel slip planes because water does not mix with PDMS and is weaker than this viscous polymer. If in nature the physical and chemical conditions are such that a weak mantle can result from transformations in the outer parts of a porphyroclast and/or can be produced elsewhere and concentrate around the rigid inclusion, then a σ-clast may develop with characteristics similar to our model: straight external surfaces of tails of material weaker than the matrix that work as local shear planes parallel to the shear plane.

4.3. Tail geometry in the non-slipping mode

Our experimental results in this mode show that a σ-inclusion is always produced if the mantle behaves similarly to the matrix (passive flow) and has a thickness such that part of it constantly lies outside the separatrix. Conversely to the slipping mode, the shape of the external surfaces of the tails in the non-slipping mode is always curved, reflecting the shape of the streamlines outside the separatrix and close to the inclusion (compare Figs. 2 and 4). The material points in the matrix very near to, but outside, the separatrix that shows drag around the inclusion in the open flow paths. Conversely, the matrix far away from the rigid inclusion runs parallel to the far field streamlines. For example, in Fig. 1B, let a point *a* on the open flow line outside the separatrix reach point *c* with progressive deformation. The flow line *a*–*c* shows drag around the rigid inclusion, with a deflection towards the reference plane, which generates the external embayments observed in the model. These cannot cross the reference plane or the separatrix. Point *b*, on the other hand, lies where streamlines are parallel to the far field flow and thus runs parallel to the shear wall to reach point *d*. Therefore, the development of σ-inclusions with external planar surfaces away from the reference plane is almost impossible in the non-slipping mode and with a mantle rheologically similar to the matrix, unless the width of the mantle is constant and very large (greater than the rigid inclusion diameter).

Our experimental results show that rigid inclusions need to be adherent to the matrix to develop δ-clasts, because there must be drag at the inclusion surface to make the mantle follow clast rotation and produce the typical external embayment that crosses the reference plane. Our experiments show that, to obtain δ-inclusions, the rate of mantle production around the inclusion must be heterogeneous, in contrast to the case of σ-inclusions. Two main cases can be analysed: (i) instantaneous mantle production, similar to the experiments of Passchier and Simpson (1986), which is a situation that should not be common in nature because it would need very particular physical and chemical conditions to be realized; and (ii) heterogeneous mantle production rate. In both cases, with progressive deformation all mantle material ultimately comes inside the separatrix and rotates continuously with the rigid inclusion (drag) in the elliptical closed paths. The mantle segments that were initially outside the separatrix track the open flow paths. The differential drags of the mantle material in the open (early stages) and closed (late stages) flow paths lead to the development of a δ-inclusion.

Although we have not worked with the eye-shaped flow pattern, we can analyse the development of tails from the theoretically derived flow lines (see fig. 4B of Masuda and Mizuno, 1996b) and compare with our results with a bow tie-shaped pattern in the non-slipping mode. In both flow types, material points outside or inside the separatrix cannot cross this boundary or any other displacement paths during deformation (they follow streamlines by definition). Therefore, σ- and δ-inclusions must always develop stair-stepping, even if in the eye-shaped flow it is very small.

5. Geological significance

Can we use our experimental models as a guide to understand natural occurrences? We believe that the examples illustrated in Figs. 5 and 6 are very good candidates as possible natural analogues of our experiments.

The degree of curvature of external embayments in σ-clasts could give us a hint as to the degree of adherence of a rigid body to the surrounding matrix and/or size of mantle. The σ-type porphyroclast systems illustrated in Fig. 5 could be very good natural counterparts of our experiments: the white mantles around the rigid porphyroclasts develop into tails that show considerable stair-stepping, but different curvature. If our experiments have any significant relationship with nature, these features could indicate low adherence of clast to matrix in Fig. 5A, and higher adherence of clast to matrix in Fig. 5B, deduced from the degree of curvature: the higher the viscous drag, the greater the tail curvature as in the model.

If we consider the reference plane (Passchier and Simpson, 1986) in the experiment to be the shear plane and in the natural occurrence to be the mylonitic foliation (also shear plane), then comparison of experimental (Fig. 4B) and natural δ-clasts (Fig. 6A) shows that: (i) median lines of both cross the reference plane as expected in a δ-clast; (ii) stair-stepping in both is prominent; (iii) in the natural δ-clast, tails are curved close to the clast but, at a short distance (one clast diameter), becomes straight and parallel to the mylonitic foliation; (iv) in the experiment, they are curved close to the clast and become straight at a short distance from it, but not parallel to the reference plane. This is because material in the tails must follow streamlines, which are not parallel to the shear plane at a short distance from the clast (cf. streamlines in Fig. 2B). Deformation was not enough to make them parallel to the reference plane, which happens far from the clast. What can we deduce from this major difference? On the one hand, in our experiments the slipping mode is the only one that produces straight streamlines parallel to the shear plane at a short distance from the clast, and, therefore, straight external surfaces of tails parallel to the shear direction close to the inclusion. On the other hand, the metamorphic record of the natural occurrence (see Marques et al., 1996) shows that it was

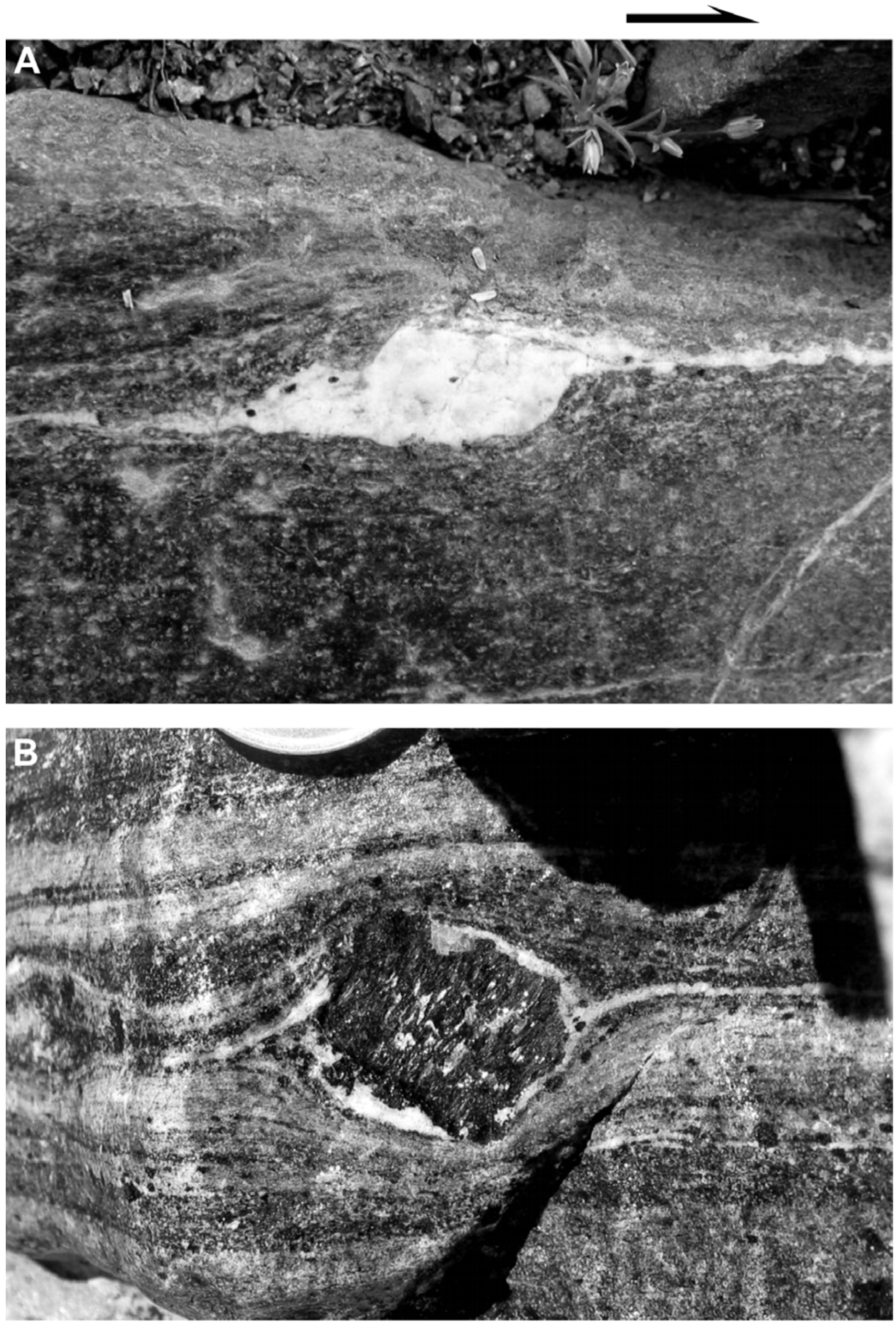

Fig. 5. Photographs of *XZ* sections of σ-clasts in natural mylonites. The great difference in shape of foliation close to clast and geometry of the tails between (A) (both rectilinear) and (B) (both curved) could be related to, respectively, lower or higher degrees of adherence of inclusions to the matrix. Note the absence of white mantle in the top left and bottom right edges of the porphyroclast in (B), which could be indicative of the position of the maximum contraction in the matrix.

sheared during exhumation of lower crustal and upper mantle rocks, with retrogression from HP–HT granulite to low amphibolite facies conditions. Therefore, our interpretation is that it is possible that during the higher temperature deformation, the clast in Fig. 6A was a slipping σ-clast like the ones in Figs. 2A and 3. Later, at lower temperatures, two simultaneous factors may have changed the geometry of the porphyroclast system: (i) friction between the clast and mylonitic matrix may have increased significantly, and (ii) considerable decrease in mantle production rate (which brought it inside the separatrix) and clast rotation dragged the tail to its present δ-geometry.

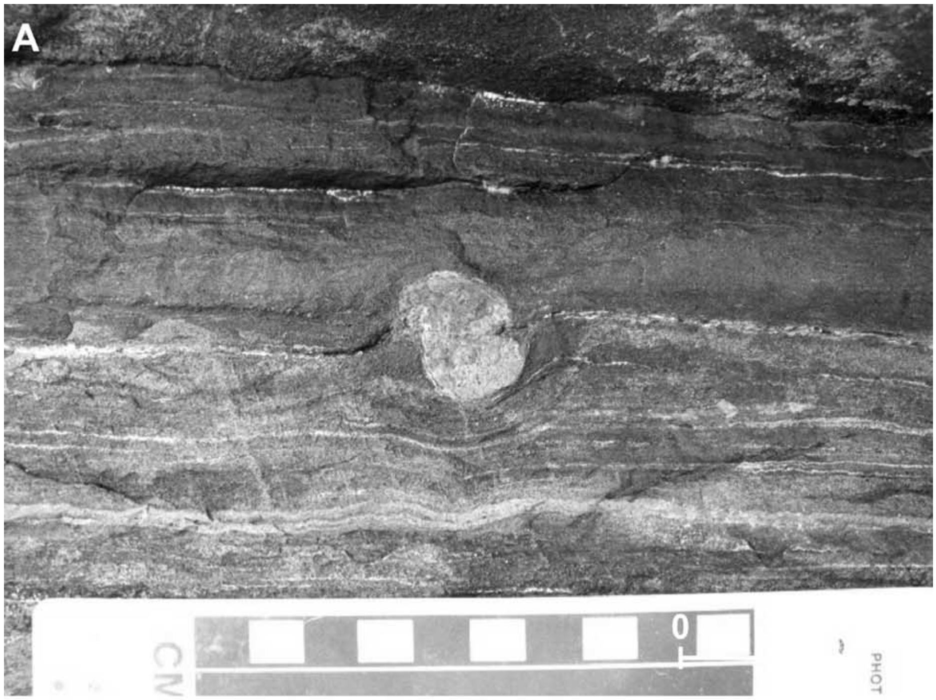

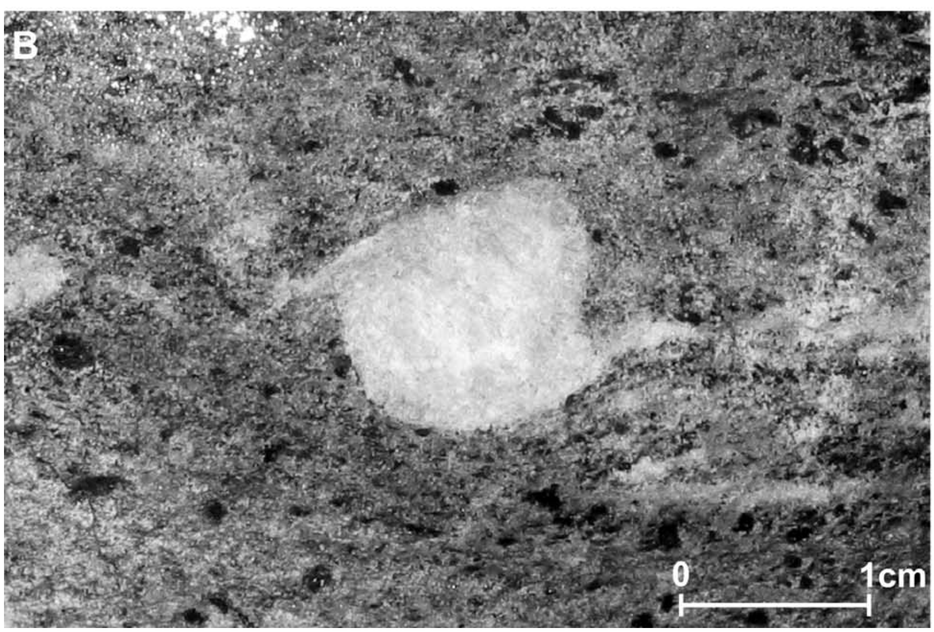

Fig. 6. Photographs of *XZ* sections of δ-clasts in natural mylonites. (A) The straight and shear parallel tails very close to the clast could, in our interpretation, indicate an early stage of σ-geometry of a clast decoupled from the matrix. (B) Plagioclase porphyroclast with δ-shape and short tails. Comparison with fig. 1 of Masuda and Mizuno (1996a) for $R=1.13$ could indicate that the mantle has remained permanently inside the separatrix in the non-slipping mode.

We have not investigated the geometry of tails when the mantle is thin enough to lie entirely within the separatrix, but Masuda and Mizuno (1996a, see their fig. 4) showed, numerically, that a δ-inclusion may also form under these conditions. Fig. 6b shows a possible natural example of such a structure, observed in high-grade metamorphic rocks of the highest allochthonous unit of the Bragança Massif, NE Portugal (see Marques et al. (1996) for the geological setting).

To summarise, we may say that experimental tails and flow patterns seem to show that a major controlling factor in the tail geometry is the position of the mantle relative to the separatrix: (i) if the mantle lies always outside the separatrix, a σ-clast forms; (ii) if the mantle lies always inside the separatrix, a δ-clast develops with very short tails that lie inside the closed streamlines; (iii) if the mantle lies outside the separatrix in the early stages of deformation and later comes inside that line, a δ-clast forms with long tails.

If our experimental results can be applied to nature, they suggest that the relatively low abundance of δ-inclusions compared with σ-inclusions in natural shear zones should not necessarily indicate that the finite deformation was low. σ-inclusions can be very abundant because, as already discussed above, they can develop in low or high finite strains, if the mantle lies outside the separatrix and its rate of production is constant, and/or if the rigid body is non-adherent to the matrix. On the other hand, the present work shows that the development of δ-inclusions is restricted to the non-slipping mode and to heterogeneous mantle production that brings the mantle inside the separatrix. The present study can, therefore, provide a possible answer to a long-standing question, which is why σ-inclusions are much more abundant than δ-inclusions in natural shear zones.

6. Conclusions

The experimental investigation of factors controlling tail geometry of porphyroclast systems in rigid-inclusion/viscous-matrix systems shows that:

1. The flow of a viscous Newtonian matrix around a rigid circular inclusion in the slipping mode is neither bow tie nor eye-shaped.
2. In the slipping mode, streamlines and passive marker lines show a rectilinear character parallel to X near the inclusion crests, in marked contrast to the perturbation of those lines in the non-slipping mode, which reflects the dominant effect of viscous drag in this mode.
3. In the non-slipping mode, a constant mantle production rate that keeps it partly outside the separatrix produces σ-systems in viscous simple shear.
4. Rigid inclusions need to be adherent to the matrix to develop δ-inclusions, because there must be drag close to the inclusion surface to produce the characteristic features of a δ-inclusion. δ-systems are born from either instantaneous or heterogeneous rates of mantle production, in contrast to σ-inclusions. In the first case, the δ-clast has this geometry since very early in the deformation history. In the latter, the mantle is initially outside the separatrix and later comes inside this line, which means that the δ-inclusion first goes through a stage of σ-system.
5. The shape of the wedge in σ-systems differs depending on the degree of adherence of the inclusion to the matrix. The slipping mode seems to be the only mode capable of producing tails with flat, shear parallel external faces. In the non-slipping mode they are curved (external embayments). This is because material particles comprising the mantle have to follow streamlines that have a different configuration depending on the degree of slip.
6. Stair-stepping is a direct consequence of viscous flow around a rigid circle, independent of type of flow and separatrix, because, by definition, material points cannot cross flow lines, in particular the separatrix and the stagnation lines. Material points born outside the separatrix, at opposite crests of the rigid body, will always remain on opposite sides of the line of flow reversal (bow tie-shaped) or stagnation line (eye-shaped), defining the stair-stepping.
7. Maximum stair-stepping occurs in the slipping mode and is at least equal to the inclusion diameter.
8. The stability of dip of inclusion greatest axis (when $R>1$) together with the tail shape of σ-inclusions can give us an indication concerning the degree of adherence of the inclusion to the surrounding matrix in simple shear.

In summary, our experimental results, together with previous theoretical models (e.g. Masuda and Mizuno, 1996a,b), show that the major factors controlling tail geometry are: (i) the degree of adherence of the inclusion to the matrix, (ii) the rheological behaviour of the mantle relative to the matrix, (iii) the position of the mantle relative to the separatrix, (iv) the flow pattern in the matrix, and (v) the mantle production rate.

If our experimental results bear a significant similarity to nature, then they can be of great help in unravelling the mechanics of natural mylonite zones. Early high rates and later very low, or null, rates of mantle production can be very common in nature, as in major overthrusts that exhume deep-seated rocks, which therefore undergo retrogressive metamorphic conditions. In such cases, δ-inclusions would represent late-stage deformation, because physical and chemical conditions would not allow the formation of mantle thick enough to lie partly outside the separatrix. If in nature the physical and chemical conditions are such that a weak mantle can result from transformations in the outer parts of a porphyroclast (as in experiments of the slipping mode) and/or can be produced elsewhere and concentrate around the rigid inclusion, then a σ-clast may develop with characteristics similar to our model: straight external surfaces of tails of material weaker than the matrix that work as local shear planes parallel to the shear plane.

Acknowledgements

This is a contribution to research project GEOMODELS (PCTI/CTA/32742/99 and POCTI/CTA/38695/2001). Santanu Bose is grateful to CSIR, India, for giving him leave to carry out work at the University of Lisbon. The final version of this paper benefited from the critical reviews of T. Masuda and P. Bons, and the editorial work of J. Hippertt. Special thanks are due to Ramon Anton of Dow Corning (Barcelona, Spain) for having made possible the acquisition of the PDMS. Experiments were performed in the Experimental Tectonics Laboratory of LATTEX.

References

Arbaret, L., Mancktelow, N., Burg, J.-P., 2001. Effect of shape and orientation on rigid particle orientation and matrix deformation in simple shear flow. Journal of Structural Geology 23, 113–125.

Bjørnerud, M.G., Zhang, H., 1995. Flow mixing, object-matrix coherence, mantle growth and the development of porphyroclast tails. Journal of Structural Geology 17, 1347–1350.

Bons, P.D., Barr, T.D., ten Brink, C.E., 1997. The development of δ-clasts in non-linear viscous materials: a numerical approach. Tectonophysics 270, 29–41.

Burg, J.-P., Iglesias, M., Laurent, P., Matte, P., Ribeiro, A., 1981. Variscan intracontinental deformation: The Coimbra–Cordoba shear zone (SW Iberian Peninsula). Tectonophysics 78, 161–177.

Ceriani, S., Mancktelow, N.S., Pennacchioni, G., 2003. Analogue modelling of the influence of shape and particle/matrix interface lubrication on the rotational behaviour of rigid particles in simple shear. Journal of Structural Geology 25, 2005–2021.

Choukroune, P., Gapais, D., Merle, O., 1987. Shear criteria and structural symmetry. Journal of Structural Geology 9, 1347–1350.

Cox, R.G., Zia, Y.Z., Mason, S.G., 1968. Particle motions in sheared suspensions. XXV. Streamlines around cylinders and spheres. Journal of Colloid Interface Science 27, 7–18.

Hanmer, S., Passchier, C.W., 1991. Shear sense indicator: a review. Geological Survey of Canada Paper 90-17.

Ildefonse, B., Mancktelow, N.S., 1993. Deformation around rigid particles: the influence of slip at the particle/matrix interface. Tectonophysics 221, 345–359.

Mancktelow, N.S., Arbaret, L., Pennacchioni, G., 2002. Experimental observations on the effect of interface slip on rotation and stabilisation of rigid particles in simple shear and a comparison with natural mylonites. Journal of Structural Geology 24, 567–585.

Mandal, N., Samanta, S.K., Chakraborty, C., 2000. Progressive development of mantle structures around elongate porphyroclasts: insights from numerical models. Journal of Structural Geology 22, 993–1008.

Marques, F.O., Bose, S., 2004. Influence of a permanent low-friction boundary on rotation and flow in rigid inclusion/viscous-matrix systems from an analogue perspective. Tectonophysics 382, 229–245.

Marques, F.G., Cobbold, P.R., 1995. Development of highly non-cylindrical folds around rigid ellipsoidal inclusions in bulk simple shear: natural examples and experimental modelling. Journal of Structural Geology 17, 589–602.

Marques, F.O., Ribeiro, A., Munhá, J.M., 1996. Geodynamic evolution of the Continental Allochthonous Terrane (CAT) of the Bragança Nappe Complex, NE Portugal. Tectonics 15, 747–762.

Marques, F.O., Coelho, S., 2001. Rotation of rigid elliptical cylinders in viscous simple shear flow: analogue experiments. Journal of Structural Geology 23, 609–617.

Masuda, T., Ando, S., 1988. Viscous flow around a rigid spherical body: a hydrodynamic approach. Tectonophysics 148, 337–346.

Masuda, T., Mizuno, N., 1996a. Computer modelling of mantled porphyroclasts in Newtonian and non-Newtonian simple shear viscous flows. Journal of Structural Geology 18, 1487–1491.

Masuda, T., Mizuno, N., 1996b. Deflection of non-Newtonian simple shear flow around a rigid cylindrical body by the Finite Element Method. Journal of Structural Geology 18, 1089–1100.

Passchier, C.W., 1994. Mixing in flow perturbations: a model for the development of mantled porphyroclasts in mylonites. Journal of Structural Geology 16, 733–736.

Passchier, C.W., Simpson, C., 1986. Porphyroclast systems as kinematic indicators. Journal of Structural Geology 8, 831–844.

Passchier, C.W., Sokoutis, D., 1993. Experimental modelling of mantled porphyroclasts. Journal of Structural Geology 15, 895–909.

Passchier, C.W., ten Brink, C.E., Bons, P., Sokoutis, D., 1993. (objects as a gauge for stress sensitivity of strain rate in mylonites. Earth and Planetary Science Letters 120, 239–245.

Pennacchioni, G., Fasolo, L., Cecchi, M.M., Salasnich, L., 2000. Finite-element modelling of simple shear flow in Newtonian and non-Newtonian fluids around a circular rigid particle. Journal of Structural Geology 22, 683–692.

Rosas, F.M., Marques, F.O., Luz, A., Coelho, S., 2002. Sheath folds formed by drag induced by rotation of rigid inclusions in viscous simple shear flow: nature and experiment. Journal of Structural Geology 24, 45–55.

Samanta, S.K., Mandal, N., Chakraborty, C., 2003. Flow patterns around rigid inclusions in a multiple inclusion system undergoing bulk simple shear deformation. Journal of Structural Geology 25, 209–221.

Schmid, D.W., 2002. Finite and infinite heterogeneities under pure and simple shear. Unpublished Ph.D. thesis, ETH Zurich, Switzerland

Simpson, C., Schmid, S.M., 1983. An evaluation of criteria to deduce the sense of movement in sheared rocks. Bulletin of the Geological Society of America 94, 1281–1288.

ten Brink, C.E., Passchier, C.W., 1995. Modelling of mantled porphyroclasts using non-Newtonian rock analogue materials. Journal of Structural Geology 17, 131–146.

Tullis, J., Yund, R.A., 1985. Dynamic recrystallization of feldspar: a mechanism of ductile shear zone formation. Geology 13, 238–241.

van den Driessche, J., Brun, J.P., 1987. Rolling structures at large shear strains. Journal of Structural Geology 9, 691–704.

Weijermars, R., 1986. Flow behaviour and physical chemistry of bouncing putties and related polymers in view of tectonic laboratory applications. Tectonophysics 124, 325–358.